CEPC NOTE

April 16, 2018

中国科学院高能物理研究所
Institute of High Energy Physics
Chinese Academy of Sciences

Higgs Decay Channels Measurement at 240Gev and 250Gev

Yongfeng Zhu

Abstract

The Circular Electron Positron Collision(CEPC) as a Higgs/Z factory is proposed by Chinese high energy physics community. So far, tests of Higgs coupling with SM particles are consistent with SM predictions.In this note, with CEPC operated at 240GeV center of mass energy, the distribution of the reconstructed invariant mass of the Higgs boson at the $\nu\nu H, H \rightarrow bb, cc, gg, \mu\mu, \gamma\gamma, ZZ^{*} and WW*$ events are shown ,and we have compared the distribution with CEPC operated at 250GeV.

E-mail address: li.gang@mail.ihep.ac.cn

Contents

1 Introduction

The standard Model of particle physics has been tested by many experiments over the last four decades and has been shown to successfully describe high energy particle interactions..However, the mechanism that breaks electroweak symmetry in the SM has mot been verified experimentally.This mechanism, which gives mass to massive elementary particles, implies the existence of a scalar particle, the SM Higgs boson.The discovery of a 125Gev Higgs boson at LHC in 2012 will possible complete the Standard Model if this boson is the Higgs.This note is organized as follows. Section 2 introduce the samples used in this note and section 3 shows the reconstruction result of the Higgs boson signals using the simulated samples of Higgs several decay modes with CEPC operated at 240GeV and 250GeV center of mass energy. The summary is given in section 4.

2 Samples

The samples we use in this note are $e^+e^- \to \nu\nu H$ with the initial state radiation and with the Higgs further decay $H \to bb, cc, gg, \mu\mu, \gamma\gamma, ZZ^* and WW*$ have been generated in the program package of Whizard 1.95. We simulated 10K events for each Higgs decay mode with Mokka, the Geant 4 simulation package for CEPC detector optimization study. The detector geometry we used in simulation is the $CEPC\_v4$ detector model, the conceptual CEPC detector evolution from $CEPC\_v1$. The default reconstruction algorithm of the CEPC software chain is based on the Arbor, a particle flow algorithm developed for the CEPC study, it attempts to identify and reconstruct all the final state particles in the most suited sub-detector systems. Explicitly, Arbor reconstructs charged particles in the tracking system, photons in the ECAL and neutral hadrons in the whole calorimeter.

3 Reconstruction results

3.1 Higgs→ $\gamma\gamma$

For the signal in the $\nu\nu\gamma\gamma$ final state channel, which has concluded both of the $e^+e^- \to ZH \to \nu\nu\gamma\gamma$ and $e^+e^- \to \nu_e\nu_e H \to \nu_e\nu_e\gamma\gamma$ channels. Considering the low branch ration of $Higgs \to \gamma\gamma$, which reaches a maximum value of 0.23% at $M_{Higgs} = 125GeV$ and falls steeply to values less than 1% above 150GeV, the performance required in photon reconstruction and energy resolution is a challenge for the Ecal design. Since photons could be easily identified from other particles, this channel is a golden channel to study properties of Higgs.

A simulation sample of 10000 $Higgs \to \gamma\gamma$ events is used to measure the Higgs boson mass. In the calculation of M($\gamma\gamma$), the energy of reconstructed photons is calibrated using their truth energy. This reduces the bias of Higgs mass measurement. The mass spectrum is fitted by a Gaussian function within the range from 118 to 132GeV to retrieve the Higgs mass mean value and width. We can draw the relationship between reconstructed Higgs mass with the transverse momentum of initial state radiation(ISR) called ISRPt to select ideal events influenced less from ISR. From the middle graph of Figure 1, we can see that the reconstructed Higgs mass would decrease with the value of ISRPt reaches 1GeV.So we can select events with ISRPt less than 1GeV. The left graph of Figure 1 shows the reconstructed Higgs mass before event selection, the right show after event selection.

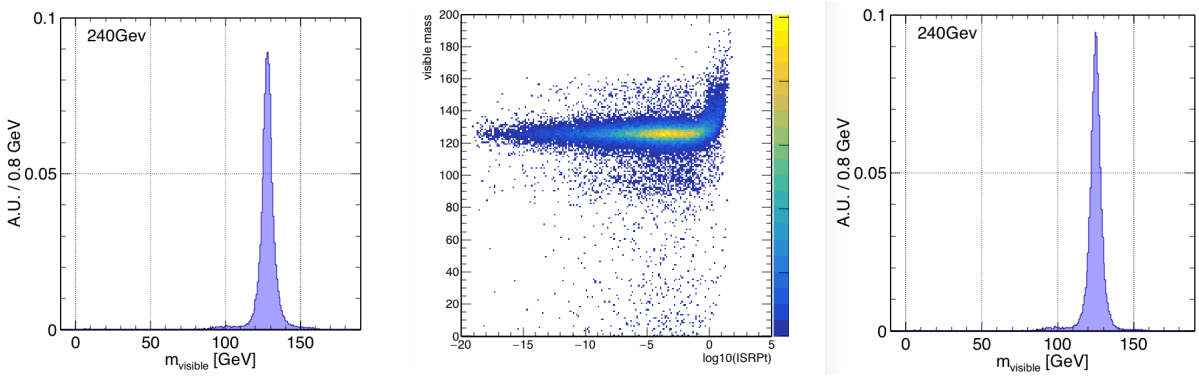

Figure 1: left graph: before events selection. right graph: after events selection

3.2 Higgs → bb, cc, gg

For a standard Model Higgs boson with a mass of 125GeV, roughly 70% of Higgs bosons decay into a pair of jetsb-quarks take up 57.8%, c-quarks take up 2.7% and gluons take up 8.6%.Measurements of these three branching ratios require efficient reconstruction of the hadronic decays of the Higgs boson.In the following, we collected all ArborPFO(final state particles) decayed from Higgs and calculate their invariant mass, which is the mass of Higgs. Before event selection, the distribution of reconstructed Higgs mass in several Higgs decay channel shown in Figure 2.

For decay of $Higgs \to gg, bb, cc$, we can also draw the relationship between reconstructed Higgs mass and several parameters, which shown as Figure 3. Then we can do some event selection to select pure event as possible as we can.

After apply the selection criteria, the distribution of reconstructed Higgs mass shown in Figure 4.

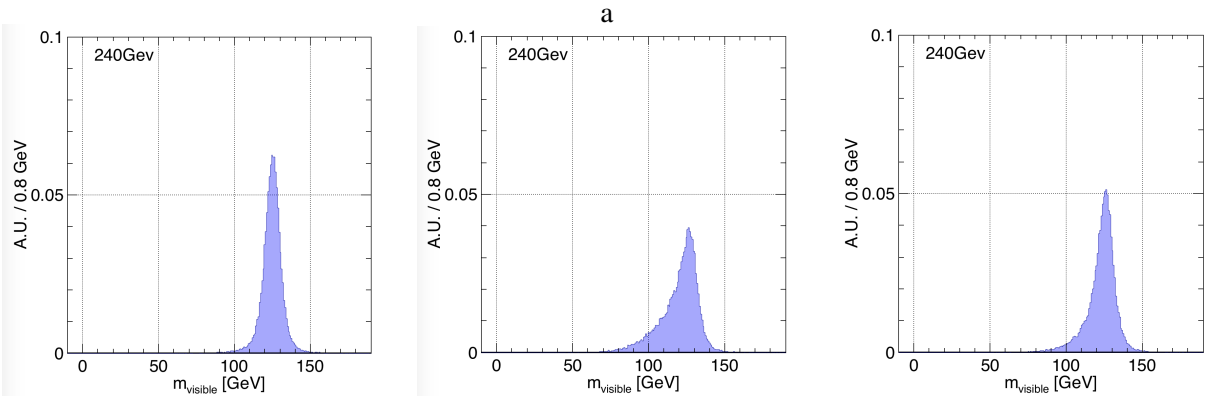

Figure 2: before event selection: left graph: *Higgs* → *gluongluon*. middle graph: *Higgs* → *bb*. right graph: *Higgs* → *cc*

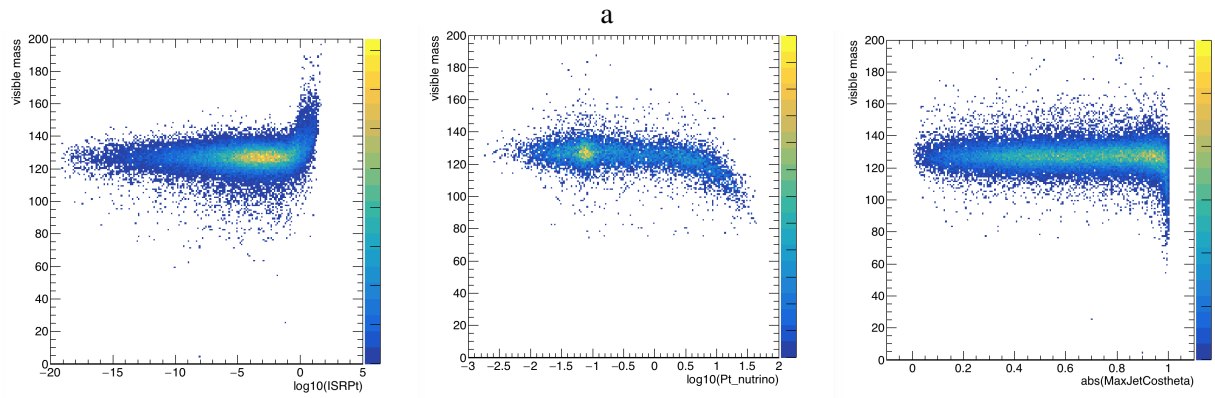

Figure 3: left graph: the relationship between reconstructed Higgs mass and the Pt of ISR photon. middle graph: the relationship between reconstructed Higgs mass and Pt of neutrino. right graph: the relationship between reconstructed Higgs mass and the angle of jets shooting the endcap

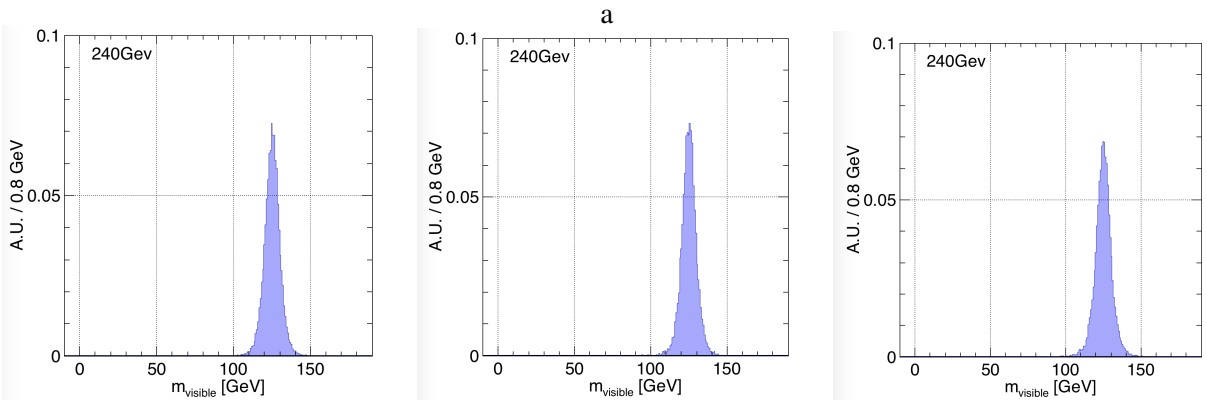

Figure 4: after event selection: left graph: *Higgs* → *gluongluon*. middle graph: *Higgs* → *bb*. right graph: *Higgs* → *cc*

3.3 Higgs → *ww*

In the SM, the branching ratio of a Higgs boson with mass 125GeV decaying to WW* is about 21.5%. We have performed a similar study on $H \to WW$ process using a simulation sample of 10000 $e^+e^- \to \nu\nu H, H \to WW$ events. We exclude the events $WW \to lvqq$ events with MC truth information since the neutrino decayed from W escape the detector and take away some energy.

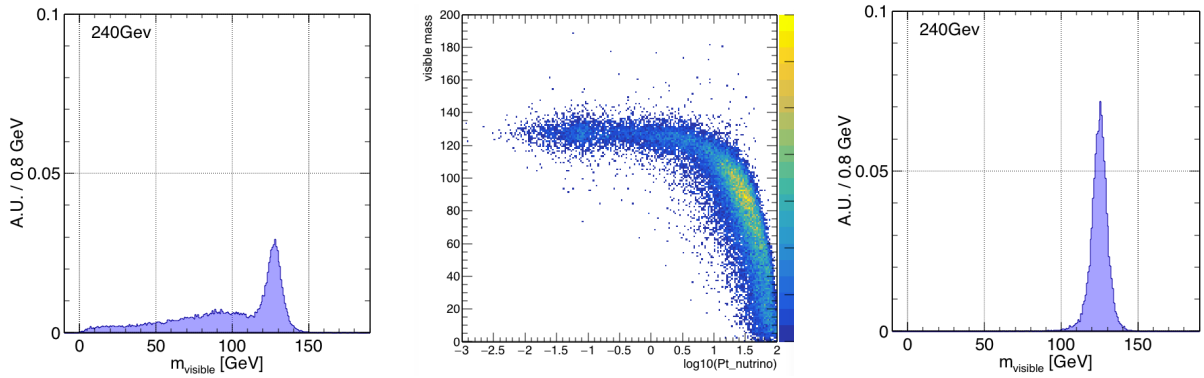

Figure 5: *Higgs* → *WW*∗ left graph: before events selection. middle graph: the relationship between reconstructed Higgs mass and the transverse momentum of neutrino. right graph: after events selection

3.4 Higgs → *zz*

The branching ratio of a SM Higgs boson at 125GeV decaying to ZZ* is about 2.64%. Limited by the Higgs mass, one of the Z boson is on shell and the other off shell. After vetoing the events with energetic, visible ISR photons, the total visible mass distribution of *Higgs* → *ZZ*∗ is shown in Figure .We can see four peaks at this distribution. The peak at zero corresponding to the total invisible decay mode where both Z and Z* decays into neutrinos. The peak at the Higgs boson mass is corresponding to the total visible mode.The other two peaks are corresponding to the conjugation case where $Z \to visible, Z* \to invisibleandZ* \to visible, Z \to invisible$. As disscussed above, we can also draw the relationship between Higgs mass and the transverse momentum of ISR photon as well as neutrino, the result shown in Figure 6. Figure 7 shows the reconstructed results before event selection and after event selection.

3.5 HIggs → *mumu*

The Higgs boson decay to $\mu^+\mu^-$ is a rare process with a branching ratio of 0.022% for a Higgs boson mass of 125GeV.

4 Summary

5 Back-Up

5.1 the comparing of reconstructed Higgs mass at CEPC between 240GeV and 250GeV

We can compare the reconstructed Higgs mass in channels of $e^+e^- \to \nu\nu Higgs, Higgs \to exclusive$ between 240GeV and 250GeV

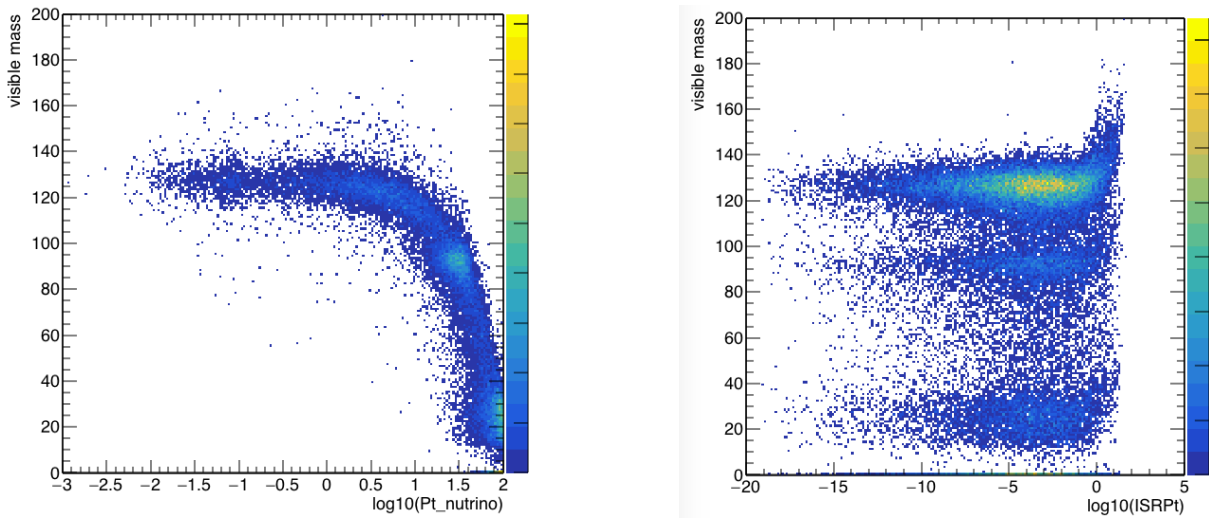

Figure 6: $Higgs \rightarrow zz$ the relationship between reconstructed Higgs mass and the transverse momentum of neutrino and ISR photon respectively

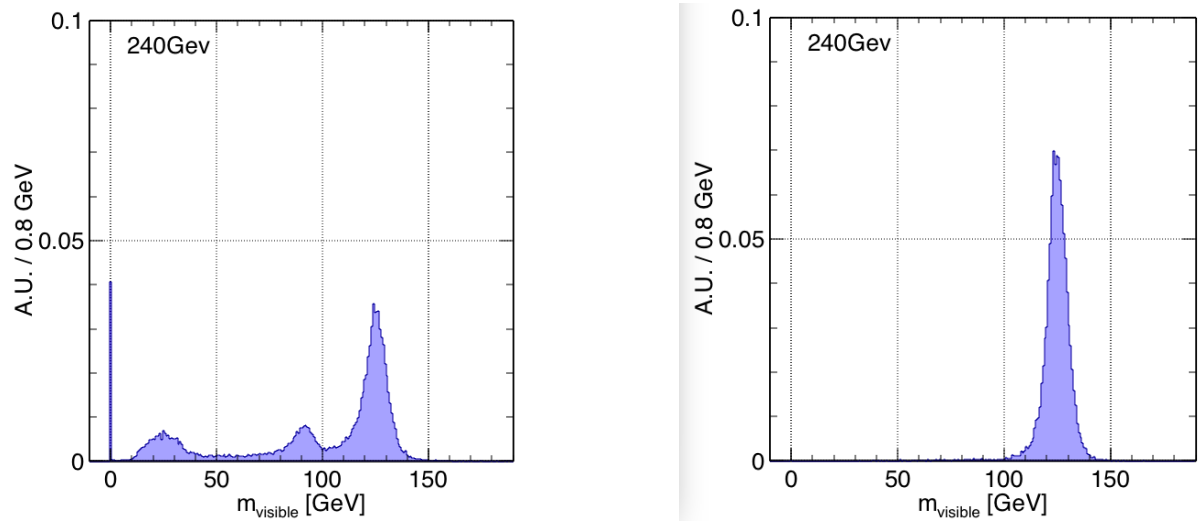

Figure 7: $Higgs \rightarrow ZZ*$ left graph: before events selection. right graph: after events selection

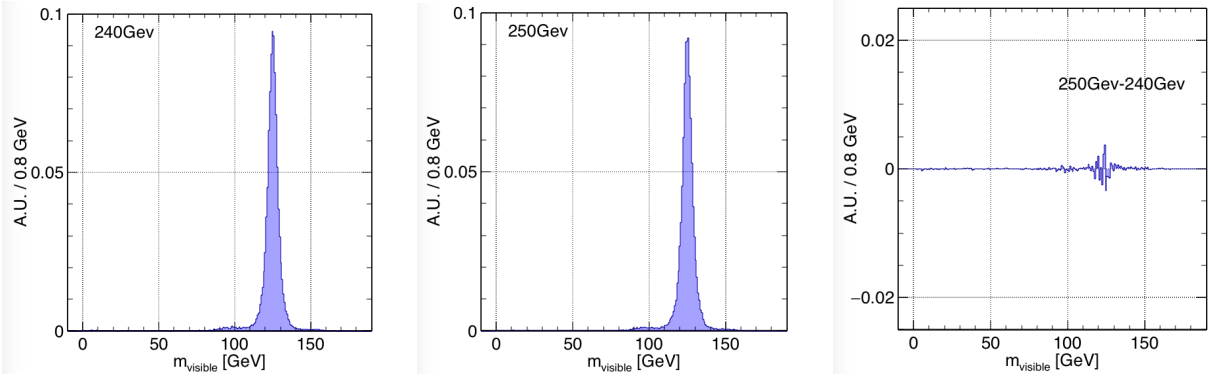

Figure 8: $Higgs \rightarrow \gamma\gamma$ left graph: CEPC operated at the center of mass 240GeV. middle graph: CEPC operated at the center of mass 250GeV. right graph: the difference between 240GeV and 250GeV

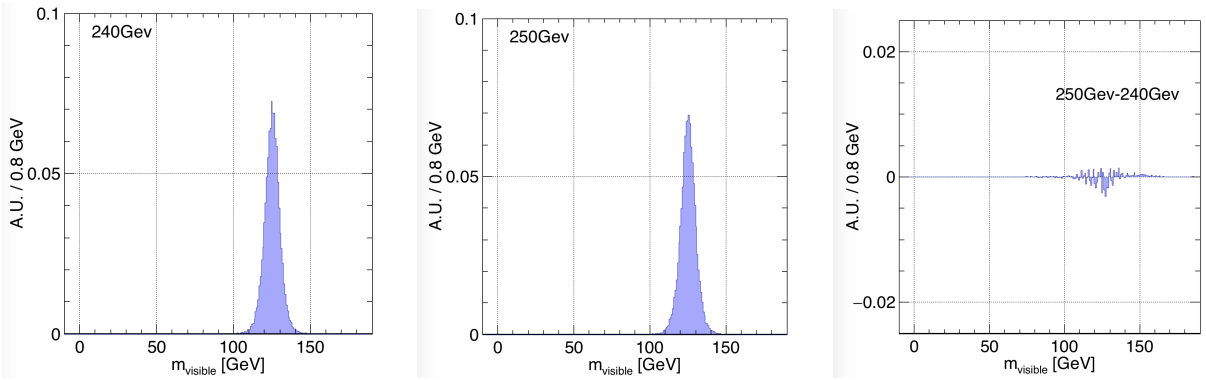

Figure 9: *Higgs* → *di* − *gluon* left graph: CEPC operated at the center of mass 240GeV. middle graph: CEPC operated at the center of mass 250GeV. right graph: the difference between 240GeV and 250GeV

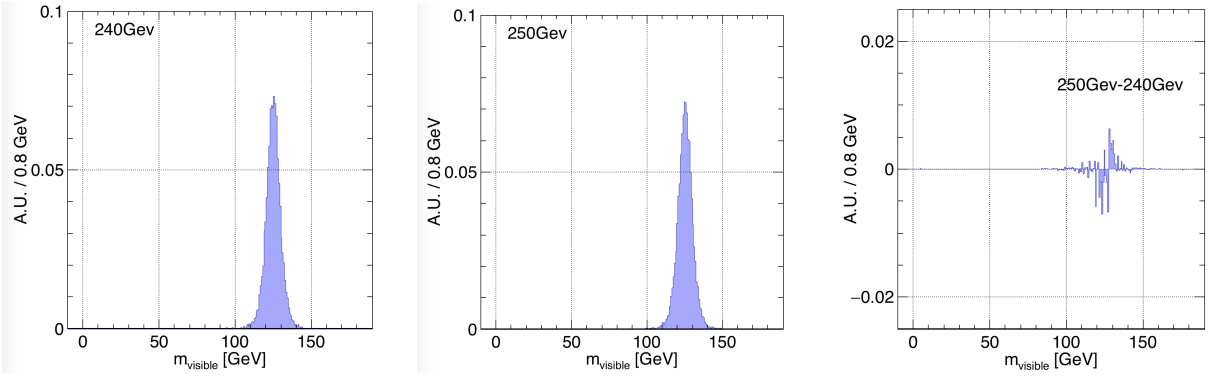

Figure 10: *Higgs* → *bb* left graph: CEPC operated at the center of mass 240GeV. middle graph: CEPC operated at the center of mass 250GeV. right graph: the difference between 240GeV and 250GeV

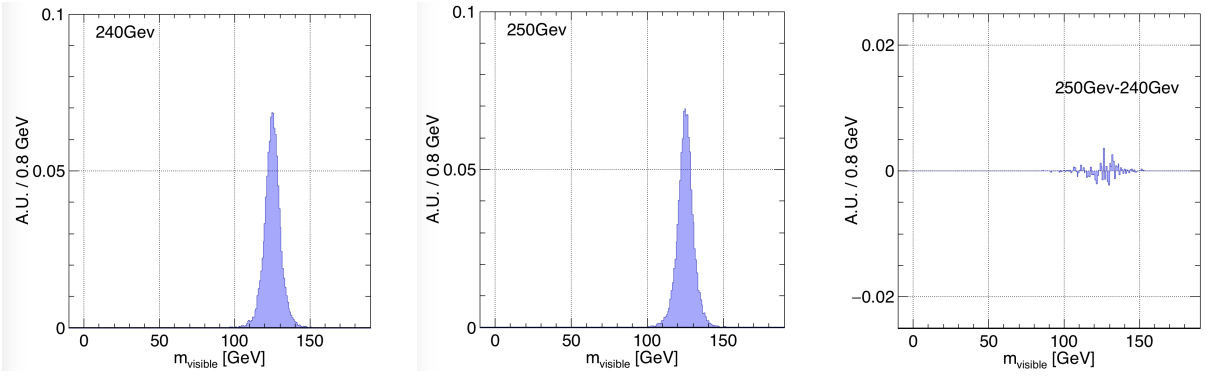

Figure 11: *Higgs* → *cc* left graph: CEPC operated at the center of mass 240GeV. middle graph: CEPC operated at the center of mass 250GeV. right graph: the difference between 240GeV and 250GeV

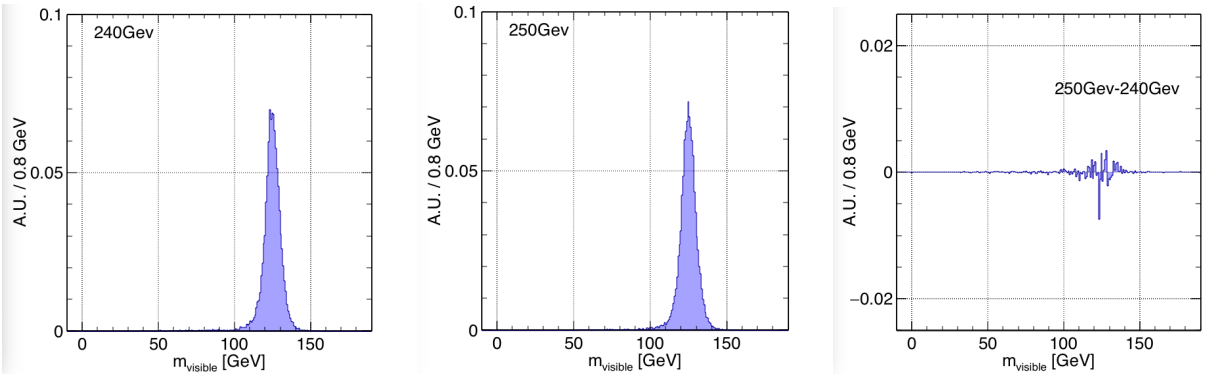

Figure 12: $Higgs \rightarrow ZZ*$ left graph: CEPC operated at the center of mass 240GeV. middle graph: CEPC operated at the center of mass 250GeV. right graph: the difference between 240GeV and 250GeV

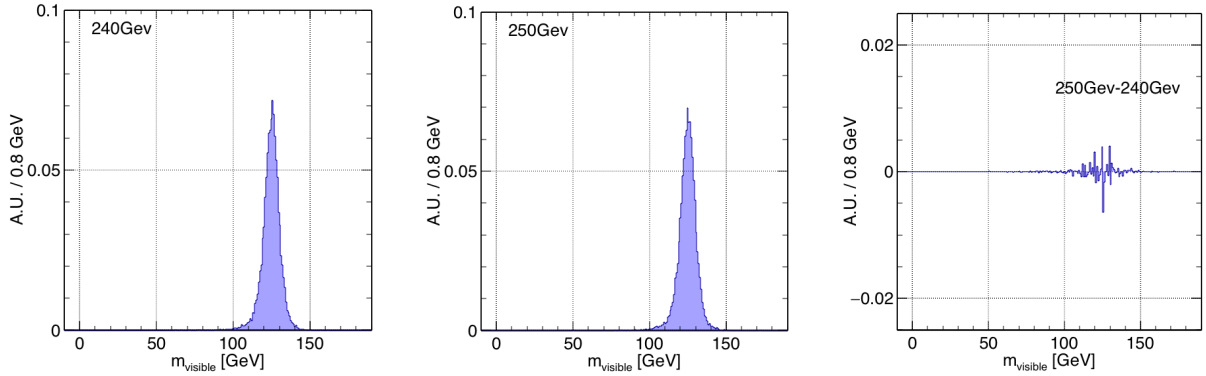

Figure 13: $Higgs \rightarrow WW*$ left graph: CEPC operated at the center of mass 240GeV. middle graph: CEPC operated at the center of mass 250GeV. right graph: the difference between 240GeV and 250GeV

5.2 the reconstructed efficiency after event selection

Table 1: The reconstructed efficiency after event selection

	$Higgs \to \gamma\gamma$	$Higgs \to bb$	$Higgs \to cc$	$Higgs \to di-gluon$	$Higgs \to ZZ*$	$Higgs \to WW*$	H
240GeV	0.9552	0.2858	0.4923	0.6727	0.4142	0.3935	
250GeV.	0.9435	0.2804	0.4784	. 0.6553	0.4024	0.3964	

6 backup

A particle shower is usually composed of a compact core and a loose halo. The core usually develops along the direction of the initial particle and contains most of the energy. The halo usually consists of many low energy clusters and isolated hits induced by secondary particles and contains minority energy of the shower. The over merging between the core and the nearby clusters could cause the confusion between showers. Giving the fact that CEPC would be operated at 91-240Gev center of mass energy, the most energetic electromagnetic particles are generated from the Bhabha events, the ISR return events and the Higgs events with Higgs bosons decay into photons. After photon energy re-calibration, the degrading induced by these geometry effects can be controlled. The CEPC detector consists if the following sub-components, a vertex detector, a silicon tracker, a time projection chamber, a calorimeter, a detector magnet system, a muon detector and a machine-detector interface. TPC has high efficiency track finding, precision momentum measurement, and low material budget. In addition, the TPC provides good dE/dx measurement, which is essential for low energy electron identification and pi-K separation.

Most of the background photons, which mainly arise from the ISR, are almost along the bean direction with lower transverse momentum. The polar angle of the ISR photons is almost around $\pm\pi$.

The photons erergy arising from higgs are high since the higgs is very heavy.So we can apply the following cuts.

This channel is sensitive to different theoretical models and new particle or physics beyond the Standard Model.

But fortunately, the Higgs boson is very rather narrow, we can try to extract the higgs signal by fitting to invariant mass of two photons if the resolution of electromagnetic calorimeter is good enough. therefor, the following optimized selection conditions are adopted.

Before reaching ECAL, the photons could also interact with the materials before ECAL.

We have found that higgs mass width has a large dependence on the fitting range, thus we have considered both the systematic and statistical uncertainties.The systematic uncertainty is estimated by varying fitting ranges from 3σ to 1.5σ. The statistical uncertainty is directly given by the fitting procedure. The total uncertainty is then quadratically compounded.

on-shell and off-shell effects in the four-fermion final states through the intermediate process of Higgs decays to heavy vector boson pair

mass shift effects in the di-photon final state due to the signal-background interference